



HAL
open science

Role of the sawtooth crash in the electron and impurity transport in the Tore Supra and JET tokamaks

T Nicolas, R Sabot, X Garbet, H Lütjens, J.-F Luciani, R Guirlet, J Decker,
A Sirinelli

► To cite this version:

T Nicolas, R Sabot, X Garbet, H Lütjens, J.-F Luciani, et al.. Role of the sawtooth crash in the electron and impurity transport in the Tore Supra and JET tokamaks. 40th EPS Conference on Plasma Physics, Jul 2013, Espoo, Finland. hal-03319518

HAL Id: hal-03319518

<https://hal.science/hal-03319518v1>

Submitted on 12 Aug 2021

HAL is a multi-disciplinary open access archive for the deposit and dissemination of scientific research documents, whether they are published or not. The documents may come from teaching and research institutions in France or abroad, or from public or private research centers.

L'archive ouverte pluridisciplinaire **HAL**, est destinée au dépôt et à la diffusion de documents scientifiques de niveau recherche, publiés ou non, émanant des établissements d'enseignement et de recherche français ou étrangers, des laboratoires publics ou privés.

Role of the sawtooth crash in the electron and impurity transport in the Tore Supra and JET tokamaks

T. Nicolas¹, R. Sabot¹, X. Garbet¹, H. Lütjens², J.-F. Luciani², R. Guirlet¹, J. Decker¹,
A. Sirinelli¹, JET EFDA Contributors*

JET EFDA, Culham Science Centre, Abingdon OX14 3DB, Oxon, England

¹ *CEA, IRFM, F-13108 Saint-Paul-Lez-Durance, France*

² *CPhT, Ecole Polytechnique, CNRS, F-91128 Palaiseau Cedex, France*

Introduction

In the Tore Supra and JET tokamaks, the plasma density equatorial profile is measured with fast-sweeping reflectometry, in ohmic sawtooth regime. The profiles are used to reconstruct the 2D density during an $(m, n) = (1, 1)$ kink mode, following the tomography technique described in Ref. [1]. Crescent-shaped structures of amplitude 1% of the total density are observed inside the $q = 1$ surface immediately following the sawtooth crash. Despite the small amplitude of the structure, it constitutes a significant deviation with respect to the expected post-crash flat profiles. In Ref. [2], this behaviour was modelled using the 3D non-linear full MHD code XTOR-2F [3]. This code is capable of simulating several self-consistent sawtooth crashes [4]. Despite full reconnection occurring in the simulation, contrary to most experimental cases, the experimentally observed density structures were recovered and it was demonstrated that they arise because of the fast flows at the reconnection layer which first advect the density along the separatrix and then reinjects it inside the $q = 1$ surface. Thus the redistribution mechanism of the density is fundamentally different from that of the temperature, the evolution of which is governed by the fast diffusive transport along the reconnected field lines. The question of the particle transport induced by the sawtooth instability has been given more importance lately due to recent experiments on the JET tokamak with the ITER like wall [5], where Tungsten (W) is seen to accumulate in the core despite frequent sawtooth crashes.

The present contribution shows JET observations of the density in ohmic regime with the same diagnostic as in Tore Supra, confirming the results of this machine, and presents results obtained with a new module of the XTOR-2F code, allowing to simulate the density evolution of several impurities considered as passive scalars, evolving in the MHD flow of the main plasma. The amount of particles reinjected inside the $q = 1$ surface, versus effectively expelled by the

*See the appendix of F. Romanelli et al., Proc. 24th IAEA Fusion Energy Conference, San Diego, USA, 2012

sawtooth crash, is determined, and conclusions are drawn.

Reflectometry results on the JET tokamak

The reflectometry technique and the subsequent tomographic inversion have recently been performed on the JET tokamak. As on Tore Supra, X-mode reflectometry is used, so that the density profile can be scanned up to the high field side, and profiles with $dn_e/dr > 0$ can be observed if $|dn_e/dr| \lesssim n_e/a$, where a is the minor radius. The results are presented in Fig. 1, which shows the density time trace and the corresponding tomographic 2D images of the density.

At the times displayed in Fig. 1,

no additional power is applied

to the plasma, so it is ohmically

heated (ICRH phase starts at $t =$

8 s). As in Ref. [2], crescent-

shaped structures following the

crash are clearly seen. In this

pulse, JET #83090, parameters

are as follows : magnetic field on

axis $B_0 = 2.55$ T, minor radius

$a = 0.95$ m, major radius $R_0 =$

2.9 m, core density $n_0 = 3.0 \times$

10^{19} m^{-3} , core electron tempera-

ture $T_{e0} = 1.8$ keV, plasma current

$I_p = 2.25$ MA, ohmic heating.

The JET density profiles were re-

constructed using the X-mode reflectometers [6]. JET reflectometers were swept simultaneously

every $15 \mu\text{s}$, this time covers the dwelt time between sweeps. 10000 profiles for a total duration

of 150 ms were recorded in the ohmic phase before heating phase.

The impurity module in XTOR-2F

The XTOR-2F code solves the MHD equations with bifluid terms included in toroidal geom-

etry. Bifluid diamagnetic terms are included in all the equations, in particular in Ohm law. The

equilibrium is provided by the CHEASE code. [7]. The equations solved by the code for the

following simulations are recalled in Ref. [2]. In order to simulate the density n_Z of an impurity

$^Z_A X$, a new equation (or as many as impurities) is added in the solver, with the following form:

$$\frac{\partial n_Z}{\partial t} + \mathbf{v} \cdot \nabla n_Z + \nabla \cdot (n_Z - n_{Z0}) \mathbf{V}_p = \nabla \cdot D_Z \nabla (n_Z - n_{Z0}), \quad k = 1, \dots, n_{imp}, \quad (1)$$

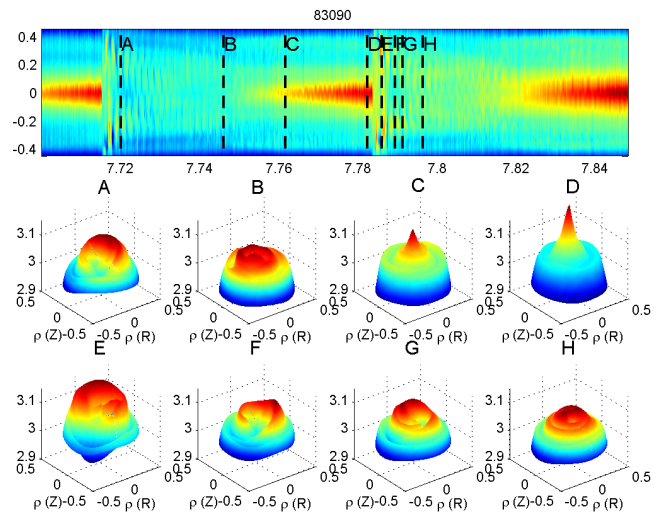


Figure 1: Time trace of the density obtained in ohmic mode inside the $q = 1$ surface, JET pulse #83090 (a) and tomography images (b)

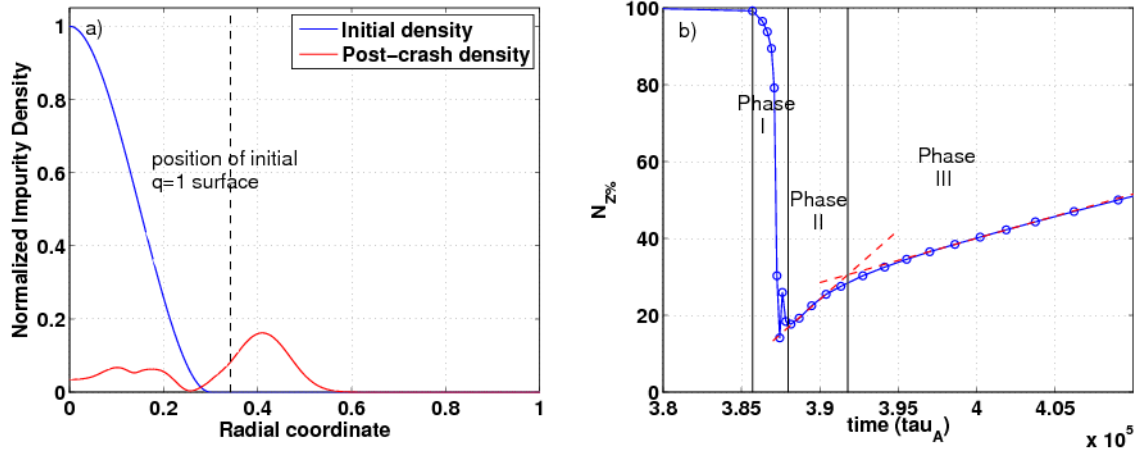


Figure 2: Density before the crash and after the crash (a), and evolution of N_Z , expressed as a percentage of the initial value (b).

where $\mathbf{V}_p = V_p(r) \mathbf{e}_r$ is the pinch velocity, $D_Z(r)$ the diffusion coefficient, $n_{Z0}(r)$ the initial density profile, and \mathbf{e}_r is the radial unit vector. Thus the only difference between the impurities lies in the choice of V_p , D_Z and n_{Z0} . The velocity \mathbf{v} is the sum of the $\mathbf{E} \times \mathbf{B}$ drift and the parallel velocity $v_{\parallel} \mathbf{B}/B$ of the plasma. Since $\nabla \cdot \mathbf{v} \neq 0$ the passive scalar assumption means there is no local conservation of particles. However (i) we checked that global particle conservation is not affected too much during our simulation (error is less than 1%) and (ii) a compressible version, including an additional equation for the parallel velocity of the impurity, is currently developed. Thus current results are only preliminary.

The choice of the initial profile and of the transport coefficients is motivated by simplicity. We aim at precisely assessing the proportion of impurities effectively ejected by the crash. The easiest way to do this is by imposing a vanishing density outside the $q = 1$ surface, and monitoring the quantity

$$N_Z(t) = \int_{\mathcal{V}_{q=1}} n_Z(\mathbf{x}, t) d^3 \mathbf{x} / \int_{\mathcal{V}_{q=1}} n_Z(\mathbf{x}, t_0) d^3 \mathbf{x}, \quad (2)$$

where $\mathcal{V}_{q=1}$ is the volume contained inside the $q = 1$ surface, and t_0 is a time immediately before the crash. The results will be expressed in percentage for convenience. In the case where impurities are efficiently expelled from the $q = 1$ surface, $N_Z = 0$ after the crash, while it has a finite value $0 < N_Z < 1$ in the opposite case. The impurity diffusion coefficient is *ad hoc* and chosen as to mimic the behaviour of critical gradient models, for example Ref. [8]. It increases by a factor of ten between the core and the edge, where it takes the value of the thermal diffusivity, $D = \chi_{\perp} = 10^{-6}$ in XTOR-2F units, normalized to a^2/τ_A , a the minor radius, τ_A the Alfvén time.

Results

Fig. 2 shows the results obtained with this method. Panel (a) shows the initial and final flux-surface averaged profiles, while panel (b) shows the evolution of $N_Z(t)$. The crash is seen to expel a significant part of the density, however the structures remaining inside the $q = 1$ surface immediately after the crash amount to approximately 15% of the total initial particle content. The post-crash profile is not flat, with a quite large hump just outside the initial $q = 1$ surface, corresponding to the mixing radius of the sawtooth. At the end of reconnection (phase I), diffusion effects take over to increase N_Z , and two slopes can be identified. In a first time (phase II) it increases quite rapidly and then more slowly (phase III). Indeed the hump diffuses both outward and inward, which contributes to increasing the particle content in the core and reducing the sawtooth efficiency. The smaller slope corresponds to the mere effect of the source.

The final value for N_Z , once the redistribution due to the crash is over (end of phase II), is around 30%, meaning that 70% only of the particle content inside the $q = 1$ surface is expelled. These results are in theory profile dependent, however similar behavior, both qualitatively and quantitatively, is recovered for all sorts of peaked profiles we have tested so far.

Conclusion

The confirmation of Tore Supra experimental results [2] on the JET tokamak and the physical analysis with XTOR-2F shows the relevance of the described structures in ohmic regime. The passive scalar study is very informative and shows that a significant part of the expelled particle content is reinjected just after the crash. This raises concern about the sawtooth flushing mechanism supposed to wash the core from impurities or He ash.

This work was supported by EURATOM and carried out within the framework of the European Fusion Development Agreement. The views and opinions expressed herein do not necessarily reflect those of the European Commission.

References

- [1] Y. Nagayama, *et al.* Rev. Sci. Instrum. **61(10, Part 2)**, 3265 (1990).
- [2] T. Nicolas, *et al.* Phys. Plasmas **19(11)**, 112305 (2012).
- [3] H. Lütjens *et al.* J. Comput. Phys. **229(21)**, 8130 (2010).
- [4] F. Halpern, *et al.* Phys. Plasmas **18(10)** (2011).
- [5] T. Pütterich, *et al.* In *24th IAEA Fusion Energy Conf., San Diego (USA)* (2012).
- [6] A. Sirinelli, *et al.* Rev. Sci. Instrum. **81(10)**, 10D939 (pages 3) (2010).
- [7] H. Lütjens, *et al.* Comput. Phys. Commun. **97(3)**, 219 (1996).
- [8] X. Garbet, *et al.* Plasma Phys. Contr. F. **46(9)**, 1351 (2004).